On-Body Detection for Today's Wearables By Exploiting Creeping Waves

***Abstract*—The ability of detecting which wearables and smartphones are on the same body has the potential to support a wealth of applications, including user authentication, automatic data synchronization, and personalized profile loading. Despite recent advances in automatic pairing and user recognition, these approaches require special sensors or dedicated hardware that cannot support versatile wearables. This paper presents the first step toward filling this gap, by creating a virtual "on-body detection sensor" based on the inherent wireless capabilities in most commercial wearables and smartphones. We investigate using the peculiar propagation characteristics of on-body creeping waves to discern on-body wearables. To this end, we decompose signals into multiple independent components to exploit the variation features of creeping waves. We implement our system on commercial off-the-shelf (COTS) wearables and a smartphone. Extensive experiments are conducted in a lab, apartments, malls, and outdoor places, involving 12 volunteer subjects of different age groups, to demonstrate the robustness of our system. Results show that our system can identify on-body devices with 92.3% average true positive rate and 5% average false positive rate.**

I. Introduction

Smart wearable devices have drawn extensive attention as they provide users continuous services, and make them interaction frictionless. A key feature desired by wearables is providing unobtrusive experience to users. Today's wearables have successfully realized the functions of automatically and continuously monitoring users' physical activities and vital signs, without interrupting the users. Recent advances in wearable computing has transformed traditionally expensive and labor-intensive tasks such as physical analytics [1] and pedestrian assistance [2], into easy processes with only unobtrusive interactions.

Existing efforts in developing unobtrusive wearables have focused on the computing dimension, while the communication wise, e.g., association and authentication, still incurs manual configurations, which becomes burdensome when people use multiple wearables and share them with other persons in a household. We argue that the first step towards unobtrusive communications is the ability that a wearable/smartphone can recognize which devices are on the same body wearing it. In our vision, a user simply pick up a household-shared device (such as heart rate monitor, blood-pressure cuff, or game control) and hand it over to another household member without any other intentional actions. The device would discover which smartphone is on the same body and automatically synchronize the measured data to the wearer's personal record systems (e.g., HealthKit in iOS and Google Fit in Android), or load personalized profile. In addition, when a user accidentally wears an unverified device (e.g., other's fitness sensor or even malicious device) or leave a device unattended (e.g., a special disease sensor needs to be worn all day long), the user's smartphone or the left device would discover the anomaly and alert the user.

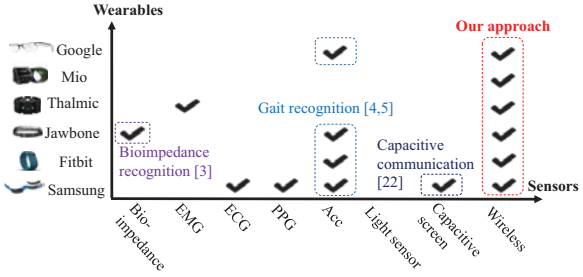

Fig. 1. Motivation of using wireless signals for on-body detection. Most COTS wearables are equipped with wireless chips.

To realize the above vision, recent advances in automatic pairing and user recognition [3]–[5] adopt special sensors, such as accelerometers and light sensors, or some dedicated hardware. They can only support a limited portion of today's wearables as the devices are equipped with a variety of sensors. One easy solution to apply these ideas to general devices is adding a dedicated sensor to each device, which, however, would be expensive: it requires wearable device manufacturers to undertake major hardware investments and also increases the hardware cost of the devices. Moreover, accelerometer-based approaches [4], [5] only work when wearers walk, and thus are unsuitable for many healthcare monitors (e.g., blood-pressure cuff).

We believe that it is essential for the on-body device detection solution to fully support versatile wearables equipped with different sensors to maximize the chance of its widespread acceptance. We observe that despite the diversity of wearables, most of them are capable of wireless connectivity, as illustrated in Fig. 1. These devices are normally connected to the wearers' smartphones for data synchronization via low-energy wireless technology such as Bluetooth. Based on this observation, we argue that instead of relying on special sensors, a better way to bring on-body detection to universal wearables is to turn the general wireless chips into "on-body detection sensors". To realize this vision, this paper presents *WeaRec*, which exploits radio propagation features obtainable in commercial wearables to recognize on-body devices.

To realize the above idea, we entail the following challenges.

1) How to exploit radio propagation features without any hardware changes to low-end wearables? Most wearables adopt Bluetooth for communication, making it inapplicable for

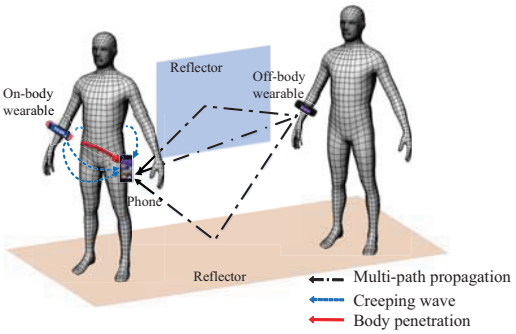

Fig. 2. Illustration of on- and off-body radio propagation. On-body propagation is dominated by creeping waves.

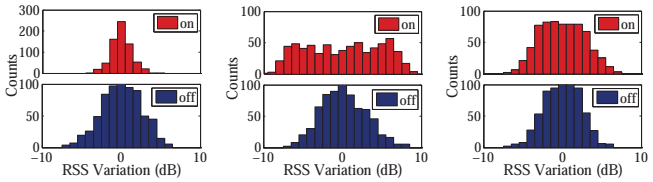

(a) Wearers are static. (b) Wearers move hands and arms. (c) Wearers move freely.

Fig. 3. Histograms of RSS amplitude of on-body and off-body devices. (a) and (b) are controlled experiments, while wearers in (c) move intermittently at their will.

them to use existing Wi-Fi-based techniques that extract signal propagation features based on fine-grained channel information [6] or even a large antenna array [7]. To overcome this predicament, our key insight is that on-body signal propagation exhibits peculiar time-domain features that lie in Bluetooth-obtainable received signal strength (RSS). As illustrated in Fig. 2, the signal propagation between a wearable device and the wearer's on-body smartphone mainly consists of *creeping waves* diffracted from human tissue and trapped along the body's surface [8]–[10], while the radio waves of general off-body links are mainly composed of direct line-of-sight (LOS) and multi-path propagations. The channel variations of creeping waves differ from off-body links in that they are less sensitive to environmental dynamics (multi-path and shadowing fading) and transmitter-receiver (Tx-Rx) distance changes (LOS path loss) [8], [11]. Thus, we can extract variations caused by different factors by decomposing received signal strength (RSS) traces into multiple independent components, and then exploit distinct variation features of creeping waves to identify on-body link.

2) How to accurately extract the desired features when signal propagation is largely affected by body motion? On-body motion severely affects creeping paths and shadowing fading, which may overwhelm the variations caused by other factors. WeaRec therefore takes a two-step approach to obtain the desired features. First, WeaRec makes an early stop to extract the direct path loss variations based on temporal and spectral properties. Then, WeaRec exploits variation patterns to find signal fluctuation periods that are likely caused by body motion, and eliminate these periods to obtain residual variations caused by environmental dynamics.

Summary of results. We implement WeaRec on a wearable system consisting of a Samsung Galaxy S4 smartphone and multiple COTS wearables, including two smart wristbands (Fitbit Force and LifeSense Mambo) and a smart waistband (Lumo Back). On the whole, WeaRec achieves an average true positive (TP) rate of 92.3% and false positive (FP) rate of 5% for 12 volunteer subjects in different indoor and outdoor environments. WeaRec can detect on-body wearables that are placed at the neck, wrist, and waist with TP rate of $90.5\% \pm 2.5\%$ and FP rate of $3.5\% \pm 1.5\%$.

Contributions. The main contributions of this work are summarized as follows. First, we show that the RSS traces obtained from COTS wearables can be utilized to detect on-body devices. Compared to previous special-sensor based approaches, its major advantage is that it can be applied to different types of wearables without any hardware changes. Second, we develop WeaRec, an on-body detection framework that can run on wearable systems consisting of COTS smartphones and wearables. The framework exploits distinct creeping wave propagation features to discern on-body devices. Finally, we test our system on 12 volunteer subjects with over 76-hour traces collected, and conduct extensive experiments in a variety of environments, including a lab, apartments, malls, and outdoor places. The results show the effectiveness of our system over different subjects, wearing positions, and environments.

II. Characterizing Radio Propagation of Wearables

A. Comparison of On- and Off-body Radio Propagation

Radio propagation is affected by direct path loss, multi-path, and shadowing fading. For off-body links, i.e., Tx and Rx are placed on different bodies with free space between them, the RSS values are governed by the Tx-Rx distance (direct path loss gain) and dynamics of the environments (multi-path and shadowing fading).

For on-body links, i.e., Tx and Rx are placed on the same body, the radio propagation exhibits different patterns: *the RSS variations have low correlations with the Tx-Rx distance and dynamics of the environments, but are highly sensitive to body motion* [11]. This is because radio waves can propagate around the body via (i) penetration path that passes through the body, and (ii) creeping path that diffracts around the body, as illustrated in Fig. 2. According to previous study [8], creeping wave plays a dominant role in on-body propagation, which indicates that on-body radio propagation is easily affected by body shape changes caused by body motion while other off-body factors such as multi-path fading have less influence.

Based on the above observations, we can exploit distinct radio propagation features to discern on-body devices. Fig. 3 shows results of a motivational experiment where each of the two users wears a COTS wristband while only one user carries a smartphone in a pocket. The RSS histograms are counted based on five-minute traces collected in a lab, where two persons keep a constant distance of 4m. When both users are static (Fig. 3(a)), the RSS amplitude of the on-body device is

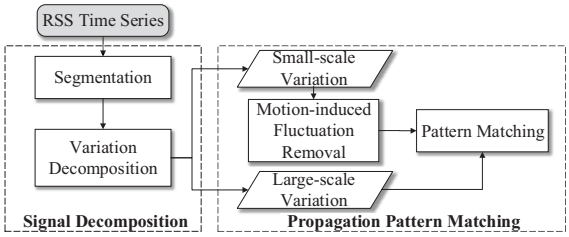

Fig. 4. System flow of WeaRec.

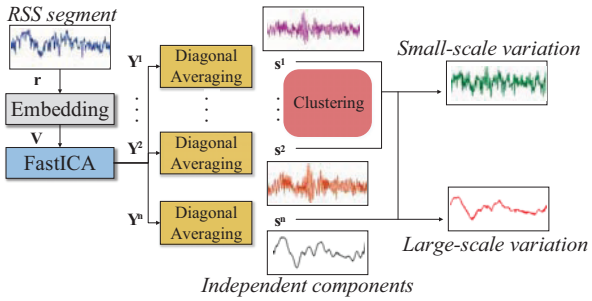

Fig. 5. Signal processing procedure of multi-scale variation decomposition.

more stable. This is because on-body propagation is dominated by the creeping path, while off-body propagation is easily affected by environmental dynamics. When users move (Fig. 3(b)), the RSS of on-body links has larger variance as the creeping path is more sensitive to changes in body shape.

B. Motivation of Decomposition

It is, however, non-trivial to directly detect on-body devices from the RSS variations. The above examples are controlled experiments where users' movements are preset, while in real cases (Fig. 3(c)) the users' motion states and the environmental dynamics are very complex and unpredictable. This makes it difficult to directly extract features from RSS variations.

Recall that the instantaneous RSS is comprised of multiple components that are caused by multiple independent factors, including Tx-Rx distance, body motion, and environmental dynamics. These factors reveal distinct patterns in on- and off-body propagations. We observe that these factors contribute to different scales of variations. Specifically, Tx-Rx distance changes are gated by the speed of human movements, and thus lead to relatively slow RSS variations (large-scale variations), while body motion such as hand gestures and environmental dynamics result in fast RSS fluctuations (small-scale variations). Therefore, we can extract desired features by decomposing the RSS time series into multiple components.

III. Design Overview

WeaRec leverages the characteristics of creeping waves to enable on-body detection on general COTS wearables with wireless capability. The crux of WeaRec is to decompose RSS traces into different levels of variations for propagation feature extraction. Fig. 4 illustrates the framework of WeaRec. It takes RSS time series as input, which is collected by a wearer's carry-on smartphone. Note that many COTS wearables (e.g., Samsung Gear Fit, Fitbit, Mio Alpha) synchronize sensor readings with connected smartphones when the corresponding smartphone applications are active. The synchronization periods of these devices are around 0.5-1.5s. WeaRec takes advantage of RSS traces from existing traffic across wearable-smartphone links. If existing traffic, which is device-dependent, is insufficient, the smartphone periodically measures RSS by sending poll packets to wearables. When there are no active sensor readings, WeaRec switches to sleep mode to save energy.

The core of WeaRec is composed of two steps, *Signal Decomposition* and *Propagation Pattern Matching*.

1) **Signal Decomposition.** WeaRec first partitions the traces into multiple basic segments. Then, WeaRec decomposes each segment into multiple independent components, and clusters them into large- and small-scale variations.
2) **Propagation Pattern Matching.** After decomposing RSS traces into different scales of variations, WeaRec eliminates the impact of body motion, and then matches the variation features of each segment to on/off-body radio propagation patterns.

IV. Signal Decomposition

The first step of WeaRec is to decompose RSS measurements into multiple components. WeaRec first divides RSS time series into segments, and then performs signal decomposition to derive multi-scale variations.

A. Signal Segmentation

A segment is the basic unit for pattern matching, and its interval should be carefully selected. If the segment interval is too long, one segment may contain both on-body and off-body states, which may mislead pattern matching. If the segment interval is too short, RSS samples in one segment may not be sufficient to extract variation features. WeaRec selects the shortest interval that provides satisfactory performance. An interval of $T = 20$s is found to be able to distinguish over 90% on- and off-body wearables.

B. Multi-Scale Variation Decomposition

Recall that the instantaneous RSS is comprised of multiple components that are caused by multiple independent factors that reveal distinct patterns in on- and off-body propagations. WeaRec aims to extract the signal variations contributed by each of these factors by decomposing the RSS time series into variations of different scales. As illustrated in Fig. 5, the signal processing procedure of multi-scale variation decomposition first separates the RSS segment to multiple independent components (Section IV-B1), and then groups them into large- and small-scale variations (Section IV-B2). The next two subsections describe the two steps, respectively.

1) Independent Component Decomposition: A direct method to derive variations of different scales is to decompose RSS traces into multiple spectral components using filters. However, it is difficult to identify the cut-off frequencies

for partitioning, as the spectral property of RSS variations varies across different environments and contexts. To address this issue, WeaRec employs single channel independent component analysis (SCICA) [12], which is widely used in biometric signal processing. The major advantages of SCICA are two-folds. First, it separates a multivariate signal into independent non-gaussian components. This fits our target of deriving multiple independent variations. Second, it requires no prior knowledge about spectral properties of components, which removes the need to set cut-off frequencies.

Generally, SCICA works by transforming a time series such that the statistical dependences between the output components are minimized. It includes three steps: embedding, separation, and recovery.

In the embedding step, an RSS segment $\mathbf{r} = [r(1), r(2), ..., r(T)]^\top$ is mapped into an $L \times K$ matrix $\mathbf{V}$, which is expressed as

$$\mathbf{V} = \begin{pmatrix} r(1) & r(2) & \cdots & r(K) \\ r(2) & r(3) & \cdots & r(K+1) \\ \vdots & \vdots & \ddots & \vdots \\ r(L) & r(L+1) & \cdots & r(T) \end{pmatrix}, \quad (1)$$

where $L = T - K + 1$ is the embedding dimension and K the number of consecutive delayed segments. The practical minimum size for L is f_s/f_l [13], where f_s denotes the sampling frequency and f_l the lowest frequency of interest in RSS signals. WeaRec sets $f_l = 0.5$Hz and adopts a larger $L = \lceil 1.5 \times f_s/f_l \rceil$ to capture substantial information from noisy and heavily correlated RSS traces.

The separation step searches for a transformation matrix $\mathbf{W}$ that decomposes $\mathbf{V}$ into multiple independent components

$$\mathbf{V} = \sum_{i=1}^{n} \mathbf{a_1}\mathbf{u_1}^\top + ... + \mathbf{a_L}\mathbf{u_L}^\top, \quad (2)$$

where $\mathbf{W} = [\mathbf{a_1}, ..., \mathbf{a_L}]^{-1}$ and $\{\mathbf{u_i} : \forall i\}$ are the independent components to be extracted. Note that we use the column vector as the default format. In our implementation, we adopt the FastICA algorithm [14] to derive $\mathbf{W}$. FastICA has the merits of fast and stable convergence, which is suitable to run on resource-limited smartphones.

FastICA treats it as an optimization problem, and iteratively estimates $\mathbf{W}$ by searching the direction that maximizes the non-Gaussianity of the projection $\mathbf{U} = [\mathbf{u_1}, ..., \mathbf{u_L}] = \mathbf{WV}$.

After deriving the transformation matrix $\mathbf{W}$, the recovery step maps $\mathbf{U}$ back to the measurement space using

$$\mathbf{Y^i} = \mathbf{a_i}\mathbf{u_i}^\top, \quad (3)$$

where $\mathbf{u_i}$ is the ith column of $\mathbf{U}$. The delay matrix $\mathbf{Y^i}$ is projected to a time series component $\mathbf{s_i}$ by applying the diagonal averaging [13], which is an inverse procedure of the embedding step.

2) Multi-Scale Variation Clustering: The obtained components $\{\mathbf{s_i} : \forall i\}$ can be quite a few (around ten components) and multiple components may associate with a single factor. Recall that we are interested in identifying variations caused by direct path loss, environmental dynamics, and body motion. Direct path loss exhibits lower frequencies of variations than the other two factors, and can thus be easily extracted from derived components. Though possessing different variations, features of environmental dynamics and body motion are harder to distinguish as both result in shadowing fading. Hence, WeaRec first extracts direct path loss variations by grouping the components into two main clusters, i.e., large-scale and small-scale variations, where large-scale variations are contributed by direct path loss.

WeaRec groups variations based on agglomerative hierarchical clustering [15], which treats each component as a singleton cluster at the beginning and then successively merges pairs of clusters until all clusters have been merged into a single cluster. The advantage of hierarchical clustering is that it stores intermediate results in the clustering procedure. For distance measure in clustering, WeaRec employs Dynamic Time Warping (DTW), a popular technique that computes an optimal match between two time series with non-linear variations [16]. The hierarchical clustering procedure successively merges clusters or components with the smallest DTW distance.

However, directly applying the DTW-based clustering does not always obtain the desired results: large-scale variations may merge with small-scale components before the final mergence, which results in a final large-scale variation cluster mixed with some small-scale components. This is because although large-scale components are quite similar under the DTW measure, the small-scale components are very diverse and some are even closer to large-scale components than the others, thereby resulting in "early mergence" between small- and large-scale components.

To address the above issue, WeaRec facilitates the intermediate results to accurately extract large-scale variations. As the spectral components of large-scale variations mainly fall into the low frequency range due to the speed limitations of human movement, WeaRec performs fast Fourier transform (FFT) to each intermediate clusters and computes the low frequency energy by summing all magnitudes in the low frequency range. Then, the large-scale variations cluster is set to be the earliest cluster that maintains a certain ratio (e.g., 0.8) of low frequency energy to total low frequency energy in the RSS segment. WeaRec sets the low frequency range to (0,1]Hz. Experiment results show we can achieve good clustering performance when the cut-off frequency is around 1Hz. In this way, WeaRec largely reduces the number of early-merged small-scale components while still preserving most large-scale variations.

WeaRec obtains the small-scale variations by subtracting large-scale variations from the RSS segment. The small-scale variations is contributed by both environmental dynamics and body motion. As both factors result in signal fluctuations that have similar frequency distributions, SCICA-based decomposition is unable to separate them. In the following section, we describe the propagation matching approach based on the obtained small- and large-scale variations.

V. Propagation Pattern Matching

After applying signal decomposition, WeaRec first exploits signal fluctuations that are likely caused by body motion, and remove them to derive residual small-scale variations. Then, WeaRec matches the variations of an RSS segment to on/off-body propagation pattern.

A. Motion-Induced Fluctuation Removal

Recall that signal fluctuations incurred by body motion overwhelm other on-body variations (Fig. 3). As we have no knowledge of the users' motion states, the motion-induced signal fluctuations can be misleading in pattern matching. To eliminate the impact of body motion, WeaRec sanitizes small-scale variations by removing the periods that contain motion-induced signal fluctuation with high probability.

From existing measurements [8], [17]–[19] and our empirical study, we observe that

- Body movements induce significant fluctuations of path gain and fading. Measurement results in many studies [8], [17], [18] have shown that signal fluctuations incurred by body motion are several times larger than those when wearers are static. Fig. 6 presents the RSS traces of an on-body device collected from the carry-on smartphone. We observe that the signal variations in hand movement period is 2-3 times larger than those in the static period.
- The frequencies of body movements fall into a low frequency range. Most frequencies of hand gestures fall into [0.3, 4.5]Hz [19], and the frequencies of other body movements are even lower. We observe that most large variations during body motion fall between 0.5Hz and 2Hz.

Based on the above characteristics, WeaRec minimizes the impact of body motion as follows. First, WeaRec applies a band pass filter to extracts spectral components of small-scale variations that fall into [0.5, 2]Hz. Then, as the lowest frequency of interest is 0.5Hz, WeaRec applies a sliding window of 2s to the small-scale variation time series, and computes the standard deviation σ_w in a window to determine whether this window contains body motion, by comparing σ_w with a threshold $\alpha\sigma$, where σ is the standard deviation of the small-scale variation time series and the coefficient α is empirically selected to be 2. After identifying the windows of body motion, WeaRec screens out these windows, and treats the residual components as the variations incurred by environmental dynamics.

B. Multi-Scale Variation Pattern Matching

So far we have obtained residual small-scale variations incurred by environmental dynamics and large-scale variations caused by direct path loss. We then exploit the features in these two scales of variations to match the RSS segment to the on/off- body propagation pattern. Recall that due to the main on-body propagation form, i.e., the creeping wave, is insensitive to direct path loss and environmental dynamics. Thus, we can discriminate the propagation patterns by examining the variations caused by these two factors.

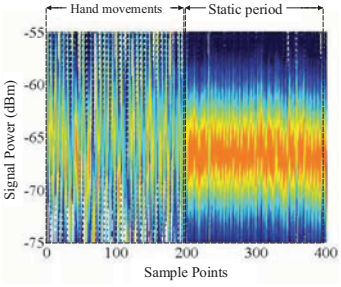

Fig. 6. Illustration of motion-induced fluctuations when the wearer moves her hands and when she keeps static, respectively.

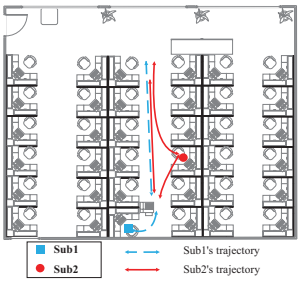

Fig. 7. Floor plan of the lab environment for benchmark experiments.

Specifically, we define a utility function that is a weighted sum of the significance of these variations:

$$u = \alpha\sigma_l + \beta\sigma_s, \tag{4}$$

where α, β are the weights for the standard deviations σ_l, σ_s of large- and small-scale variations, respectively.

To determine α, β, we adopt a heuristic approach by measuring the standard deviations in on- and off-body traces. The traces are collected over a short period of time (e.g., 15 min) in different scenarios, including malls, apartments and outdoor places. We first compute the average standard deviations $\{\bar{\sigma}_l^{\text{on}}, \bar{\sigma}_s^{\text{on}}\}$ in on-body traces and $\{\bar{\sigma}_l^{\text{off}}, \bar{\sigma}_s^{\text{off}}\}$ in off-body traces. We allocate proportionally more weights to the coefficient of which the standard deviations in the two traces have a larger difference, that is,

$$\frac{\alpha}{\beta} = \frac{\bar{\sigma}_l^{\text{on}} - \bar{\sigma}_l^{\text{off}}}{\bar{\sigma}_s^{\text{on}} - \bar{\sigma}_s^{\text{off}}}. \tag{5}$$

To match the RSS segment to on/off-body propagation pattern, we compare u with a threshold as follows

$$\begin{cases} u \geq \alpha(\bar{\sigma}_l^{\text{on}} + \bar{\sigma}_l^{\text{off}})/2 + \beta(\bar{\sigma}_s^{\text{on}} + \bar{\sigma}_s^{\text{off}})/2 & \Rightarrow \text{off-body} \\ u < \alpha(\bar{\sigma}_l^{\text{on}} + \bar{\sigma}_l^{\text{off}})/2 + \beta(\bar{\sigma}_s^{\text{on}} + \bar{\sigma}_s^{\text{off}})/2 & \Rightarrow \text{on-body} \end{cases}. \tag{6}$$

VI. Micro-Benchmark Experiments

The target of micro-benchmark experiments is to evaluate our system performance under different basic scenarios. Specifically, we evaluate our system when wearers are in 9 different motion states.

A. Experimental Setup

1) Device and System: We conduct experiments using a Samsung Galaxy S4 smartphone and two wearables, i.e., one Fitbit Force, and one LifeSense Mambo. The smartphone runs Android 4.4 firmware and is equipped with a Bluetooth 4.0 chipset to communicate with wearables at 2.4GHz. An android app is implemented on the smartphone to send poll packets to connected wearables, and log RSS measurements for offline analysis. Unless otherwise stated, the polling interval is set to 200ms. How the interval affects the performance is discussed in our results.

Sub2's state \ Sub1's state	Static	Body Motion	Walking
Static	0.89	0.79	0.93
Body Motion	0.85	0.83	0.93
Walking	0.87	0.82	0.90

(a) TP rate under various wearer motion states.

Sub2's state \ Sub1's state	Static	Body Motion	Walking
Static	0.25	0.17	0.03
Body Motion	0.29	0.14	0
Walking	0	0	0

(b) FP rate under various wearer motion states.

Fig. 8. TP and FP rates under various wearer motion states.

2) Lab Environments: Micro-benchmark experiments are conducted in a 10m×10m lab, as illustrated in Fig. 7. We present extensive evaluations of our system in real environments in Section VII. The lab consists of 36 cubics. There were 4 and 36 students in Lab1 and Lab2, respectively, with most of them sitting in front of their desks, and only a few students walking during the experiments. We conduct experiments on different days during work hours.

3) Wearer Motion States: The benchmark experiments involve two volunteers Sub1 and Sub2, and each of them wears a smart wrist band (i.e., Fitbit Force and LifeSense Mambo). Sub1 puts the smartphone in her pocket while not seated. Sub1 may hold the phone, put it in a pocket, or place it on the desk while seated. We consider 9 motion state scenarios as described in Fig. 8, where each wearer goes through the following three motion states.

- **Static.** In the Static state, the wearer sits in front of her desk and makes no body motion such as gestures and hand/arm movements. In this state, the wearer can be asleep or watching video.
- **Body Motion.** In the Body Motion state, the wearer sits in front of her desk and makes certain movements. These movements include cleaning the desk, tapping the keyboard, and other occasional hand/arm movements.
- **Walking.** In the Walking state, the wearer walks along the aisles in the lab.

We collect total 4.5-hour RSS traces for analysis, with 0.5 hour for each state combination.

4) Metrics: We use the following metrics to evaluate the performance of our system.

True positive (TP) rate. TP rate is defined to be the probability of correctly detecting the on-body wearables.

False positive (FP) rate. FP rate is the probability of falsely recognizing off-body wearables as on-body ones.

B. Results

Fig. 8 shows the TP and FP rates of our system under various wearer motion states. For all cases demonstrated in Fig. 8(a), on-body devices are correctly recognized with ratios over 79%. The average TP rates of different on-body states have the following relation: Walking > Static > Body Motion. The reason is that in the Walking state, the hand and leg movements are oscillatory, which makes it easy for WeaRec to remove body motion with high precision. In the Static state, the placements of the smartphone are versatile: it may be placed on desk, held in the hand, or put in a pocket. These different placements increase the uncertainty of the creeping wave propagation, thereby slightly dragging down the TP rate. However, WeaRec still achieves over 85% TP rate in spite of different smartphone placements. The TP rate in the Sub1 Body Motion state is lower than the others due to the imperfect removal of motion-induced fluctuation.

In Fig. 8(b), the FP rate is lower than 17% in most cases except the two cases of Sub1 being static. In the five Walking cases, WeaRec achieves very low FP rates of 0-3%, as we can exploit both large and small-scale variations to recognize the off-body wearable. The worst cases are the states where Sub1 is static while Sub2 is sitting (Body Motion and Static states). In these two cases, the small-scale variations for Sub2's device are small, and thus are easily recognized as on-body propagation. In real cases, the chance is rare for a person to continuously remain static, and thus WeaRec can still achieve a high detection accuracy. In the following section, we conduct extensive experiments to validate WeaRec in real environments.

TABLE I
BASIC INFORMATION OF VOLUNTEER SUBJECTS.

Sub.	1	2	3	4	5	6	7	8	9	10	11	12
Sex	F	F	F	F	F	M	M	M	M	M	M	M
Age	21	26	50	59	81	17	22	25	26	53	54	61

VII. Evaluation in Real Environments

In this section, we evaluate WeaRec in real environments with uncontrolled body motion. The experiments involve 12 volunteer subjects, and are conducted in apartments, malls, and outdoor places.

A. Experimental Setup

1) Enrolled Participants: We invite 12 volunteers, whose basic information is listed in Table I, to participate in the experiments. The subjects include a teenager, five college students, five middle-aged people, and an elderly. We specifically select subjects to cover different age groups and both genders. These subjects normally have different body motion patterns. The elderly moves slower while younger people move faster and are more active. The subjects also vary in height and weight, ranging from 5 to 6ft and 100 to 190lbs, respectively. The creeping wave propagations might have different patterns on people of different shapes. We intend to see whether body motion and shape affect the experimental results.

2) Methodology: To validate WeaRec in real cases, we do not control wearers' movements as in benchmark experiments. We only ask volunteers to wear the devices, and then the wearers continue their daily activities in different environments. For example, in apartments, wearers may do housework, rest, dine as usual; while in malls, wearers walk and pick up goods for shopping. Wearers are free to talk and make gestures during the experiments. Unless otherwise stated, volunteers wear the Fitbit Force or LifeSense Mambo on their wrists as the wearables, and place the smartphone in a pocket or hold it in the hand.

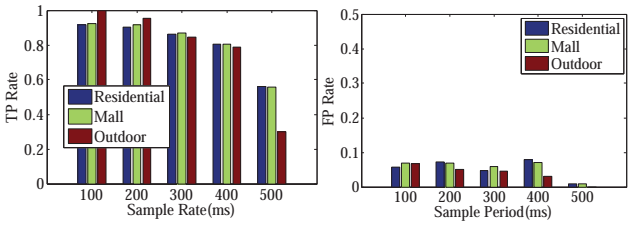

(a) TP rate. (b) FP rate.

Fig. 9. FP and TP rates under various RSS sample periods in different environments.

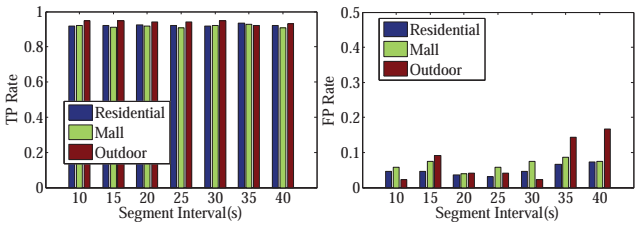

(a) TP rate. (b) FP rate.

Fig. 10. TP and FP rates under various segment intervals in different environments.

B. Evaluation in Different Scenarios

1) Environments: People wear devices in many different indoor and outdoor places. Indoor propagations significantly differ from outdoor propagations, in terms of multi-path fading, shadowing, and direct path loss. Moreover, the propagation patterns in different indoor environments (e.g., different layouts and user densities) are also versatile. It is thus important to evaluate the robustness of WeaRec in various environmental scenarios. We study the following three representative scenarios. In each scenario, two subjects wear wearables and one of them carries a smartphone.

- **Residential scenario.** We test our system in three different-sized (i.e., 1000-, 1300-, and 1600- ft^2) apartments. 2-6 other people including family members and visitors are co-located in the apartment. Wearers rest in couch, watch TV, walk, cook, and clean floors during our tests.
- **Mall scenario.** This scenario includes a small-size supermarket (about 30ft $\times$ 50ft) and a large shopping mall. The mall environments are very dynamic, with people frequently passing by. The wearers go shopping together, with a series of activities like walking, browsing, and picking up the goods involved.
- **Outdoor scenario.** The outdoor scenario includes two types of environments, i.e., plaza and walkway. In the plaza, the two wearers wander randomly, while in the walkway, the two wearers walk side-by-side along the road. In both cases, the wearers may chat with each other while making occasional gestures.

We conduct the experiments over 14 different days, and collect RSS traces of 25.01 hours, with 10 hours in the residential scenario, 6.26 hours in the mall scenario, and 8.75 hours in the outdoor scenario.

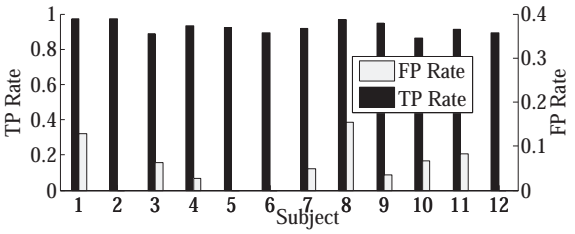

Fig. 11. Whole-day performance for different subjects.

2) Results: We evaluate the robustness of WeaRec in different environments in Fig. 9 and Fig. 10. The results show that the TP and FP rates are similar over different environments when the RSS sample period ranges from 100ms to 300ms, and the segment interval is no larger than 30s.

Fig. 9 plots the FP and TP rates of WeaRec under various RSS sample periods, where the segment interval is fixed to 20s. Higher sample rates can provide finer-grained propagation information. WeaRec achieves similar performance in the three environments. We observe that for the sample rate of 100-300ms, the TP rate is higher than 85%, and the FP rate is as low as below 8%. Wearables are likely to be classified as off-body devices (low TP and FP rates) when the sample period is larger than 400ms, as the small-scale variations are mistakenly recognized as large-scale variations with high probability due to low RSS granularity. The results indicate that WeaRec performs well with a reasonable sample period less than 400ms.

Then, we evaluate the performance of WeaRec under various segment intervals in Fig. 10, where the sample period is set to 200ms. The TP rate is insensitive to the variation in segment interval, and remains as high as over 91%; while the FP rate increases quickly when the segment interval goes over 30s. This is because the off-body pattern is more complex than on-body pattern, which increases the difficulty to precisely decompose longer off-body RSS time series. Besides, the optimal segment interval that offers the lowest FP rate in the figure is 20s, as the RSS samples in the segments with intervals less than 20s fall insufficient to perform pattern matching.

C. Whole-Day Evaluation

1) Setup: We evaluate WeaRec for whole-day (3-5 hours) activities. In each experiment set, two co-located subjects (e.g., colleagues in the same office, hang-out friends) wear wearable devices and one of them carries the smartphone that collects RSS traces. The wearers perform their daily activities as usual, including hanging out in coffee shops, shopping, driving, walking, dining, doing housework, office working, etc. The evaluation lasts 12 days, with 51.46-hour traces in total from 12 subjects.

2) Results: Fig. 11 presents the TP and FP rates for all subjects. The RSS sample period and segment interval are set to 200ms and 20s. WeaRec achieves the average TP and FP rates of 92.3% and 5%, respectively. The differences in TP and FP rates for all subjects are within 8% and 15%. The differences manly come from activity differences between

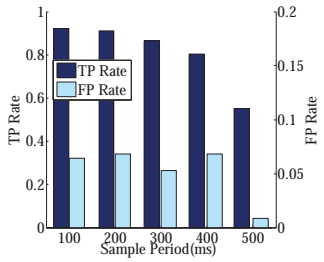

Fig. 12. Whole-day user recognition performance under various sample periods.

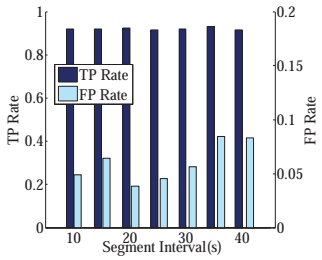

Fig. 13. Whole-day user recognition performance under various segment intervals.

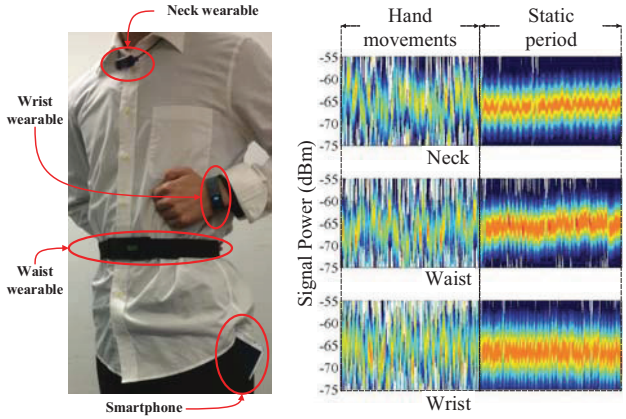

(a) Wearing positions.

(b) Illustration of RSS variations at different positions.

Fig. 14. Experiment scenario of different wearing positions. The subject wears three different wearables at neck, waist, and wrist, and carries a smartphone in pocket.

subjects. The worst TP and FP rates are 89% and 15%, which validates the effectiveness of WeaRec across different subjects.

Fig. 12 and Fig. 13 show the whole-day performance under different RSS sample periods and segment intervals. The results are consistent with Fig. 9 and Fig. 10, and demonstrate that the performance of WeaRec remains stable for both short and long-term activities.

D. Performance For Different Wearing Positions

1) Setup: Different positions on the body affect the radio propagations of wearables. We evaluate the performance for wearables at different positions. We select three typical positions for wearables, i.e., neck (smart necklace), wrist (smart wristband/watch), and waist (smart waistband). In our experiments, subjects wear a LifeSense Mambo around the neck to emulate a smart necklace, a Fitbit Force on the wrist, and Lumo Back one Lumo Back around the waist, as shown in Fig. 14(a). Two co-located subjects are involved in this experiment to wear on- and off-body devices. Subjects perform their daily activities as described in Section VII-C.

2) Results: Fig. 14(b) shows that the detailed signal variations at different positions are different, while the main feature still stands: on-body propagation is very stable when the wearer is static, yet varies significantly when the wearer moves. Table II summarizes the TP and FP results. WeaRec

TABLE II
TP AND FP RATES FOR DIFFERENT POSITIONS.

Position	Neck	Waist	Wrist
TP Rate	0.88	0.93	0.92
FP Rate	0.02	0.03	0.05

achieves $90.5\%\pm2.5\%$ TP rate and $3.5\%\pm1.5\%$ FP rate, which validates its robustness against different wearing positions.

VIII. Discussion

Energy Consumption. We log the battery life of Fitbit Force during our experiments to estimate energy consumption. We connect the Fitbit to a Samsung S4 using the WeaRec app, and observe that the fully-charged Fitbit lasts 10 days, during which the app collects RSS traces of 51 hours. Note that when the fully-charged Fitbit lasts 7-10 days when it is connected to a smartphone using the Fitbit app. This suggests that we can expect a battery life of several days when WeaRec is incorporated with the Fitbit app. For other wearables such as the Mio heart rate watch, the energy consumption would be even lower due to the short active periods. Moreover, in future backscatter-based sensing platforms [20], communication-incurred power consumption would be much lower.

Constant traffic requirement. In our experiments, WeaRec is evaluated with periodic RSS traces. WeaRec is only active to collect RSS traces from: 1) disconnected wearables that broadcast beacons, and 2) active connected devices. When wearables are inactive, no readings are generated, and thus there is no need to collect RSS for on-body detection. For disconnected wearables, the overhead of WeaRec is manageable as it works at rates (hundreds of milliseconds) that match many beaconing rates. When connected and active, many wearables (e.g., Samsung Gear Fit, Mio Alpha, Fitbit) synchronize with smartphones for a period of 0.5-1.5s. In this case, the smartphone sends poll packets once the inherent packet transmission rate is lower than expected. In future battery-free sensing platforms as envisioned in [20], the traffic requirement would be easily satisfied, as passive radios continuously forward raw data to the reader, e.g., the smartphone in our case, and generate constant traffic at extremely low cost.

Smartphone Placements. Similar to many smartphone-based approaches [4], [4], [21], we assume that each wearer carries a dedicated smartphone or places it nearby (e.g., on the wearer's desk with only tens of centimeters distance). When the smartphone is off-body, it may mistakenly recognize on-body wearables as off-body devices. To address this issue, the smartphone can incorporate a self on-body checking scheme that detects whether the device itself is on-body using motion sensors, e.g., [4]. It is noteworthy that WeaRec applies to other user-dedicated devices like smart watches or user-verification wearables [3], which are worn by users most of the time.

IX. Related Work

Sensor-based user recognition and on-body detection. The prevalence of smart devices has spurred growing attempts and extensive efforts in developing user recognition systems for new applications and human-device interactions. Specific

sensors, including bioimpedance sensor [3] and capacitive touch sensor [22], are widely used to discern which devices are on a certain body. These systems capture individual differences using different sensors, and build the basis for automatic user verification, synchronization and profile loading. Instead of using dedicated sensors, Ren et al. [4] and Srivastava et al. [5] consider on-body smartphones as identifiers for wearers, and realize the above goals by detecting devices that are on the same body carrying a smartphone. In particular, motion sensors are used to check if devices share similar footstep patterns when the wearer walks. However, motion sensor based approaches are limited to walking scenarios and fitness related wearables. Different from these systems, WeaRec aims to bring the abilities of automatic user verification, synchronization and profile loading to general COTS wearables using their built-in wireless chipsets, which are equipped in most commercial fitness, healthcare, and cognitive wearables of versatile form factors.

Automatic device pairing. Automatic device pairing frees users from cumbersome and time-consuming interactions for configuring devices. Many approaches have been proposed to connect devices with a simple gesture [23], [24] or intention [25]. These approaches pair devices based on human interactions, and thus cannot be applied in our case to automatically pair on-body devices. Miettinen et. al [26] exploit ambient context, like ambient noise and luminosity, as a co-presence evidence to provide a secure zero-interaction pairing scheme. This pairing scheme distinguish co-present devices at the room level, and thus cannot be used to discriminate multiple users in the same room or outdoor scenarios.

Body-area network (BAN) channel characterization. Many existing measurements have studied the propagation model for on-body channels [8], [11], [17], [18], [27]. These studies suggest that there exists substantial differences in on-body and off-body propagations. Their measurement results indicate that it is feasible to use radio propagations to distinguish between on-body and off-body devices.

X. Concluding Remarks

This paper presents WeaRec, a low hardware cost approach for on-body detection by extracting the distinct creeping wave propagation features of on-body devices. The insight is that on-body radio waves propagate mainly in the form of creeping waves, which have unique characteristics reflected in RSS variations. We demonstrate the generality of WeaRec by evaluating it using different COTS wearables. The experiments are conducted on 12 subjects of different age groups, and the environments cover a lab, an office, apartments, malls, coffee shops, plazas, walk ways, and so on. The results show WeaRec achieves an average TP rate of 92.3% and FP rate of 5%, and is robust for devices worn at different positions, including the neck, wrist, and waist.

References

[1] S. Rallapalli, A. Ganesan, K. Chintalapudi, V. N. Padmanabhan, and L. Qiu, "Enabling physical analytics in retail stores using smart glasses," in *Proc. ACM MobiCom*, 2014, pp. 115–126.

[2] S. Jain, C. Borgiattino, Y. Ren, M. Gruteser, Y. Chen, and C. F. Chiasserini, "Lookup: Enabling pedestrian safety services via shoe sensing," in *Proc. ACM MobiSys*, 2015, pp. 257–271.

[3] C. Cornelius, R. Peterson, J. Skinner, R. Halter, and D. Kotz, "A wearable system that knows who wears it," in *Proc. ACM MobiSys*, 2014, pp. 55–67.

[4] Y. Ren, Y. Chen, M. C. Chuah, and J. Yang, "Smartphone based user verification leveraging gait recognition for mobile healthcare systems," in *Proc. IEEE SECON*, 2013, pp. 149–157.

[5] A. Srivastava, J. Gummeson, M. Baker, and K.-H. Kim, "Step-by-step detection of personally collocated mobile devices," in *Proc. ACM HotMobile*, 2015, pp. 93–98.

[6] Y. Wang, J. Liu, Y. Chen, M. Gruteser, J. Yang, and H. Liu, "E-eyes: device-free location-oriented activity identification using fine-grained wifi signatures," in *Proc. ACM MobiCom*, 2014, pp. 617–628.

[7] F. Adib, Z. Kabelac, D. Katabi, and R. C. Miller, "3d tracking via body radio reflections," in *Usenix NSDI*, 2014, pp. 317–329.

[8] J. Ryckaert, P. De Doncker, R. Meys, A. de Le Hoye, and S. Donnay, "Channel model for wireless communication around human body," *IET Electronics letters*, vol. 40, no. 9, pp. 543–544, 2004.

[9] D. McNamara, C. Pistorius, and J. Malherbe, "The uniform geometrical theory of diffraction," *Artech House, London*, 1990.

[10] R. Pethig, "Dielectric properties of body tissues," *Clinical Physics and Physiological Measurement*, vol. 8, no. 4A, p. 5, 1987.

[11] F. Di Franco, C. Tachtatzis, B. Graham, D. Tracey, N. F. Timmons, and J. Morrison, "On-body to on-body channel characterization," in *Proc. IEEE Sensors*, 2011, pp. 908–911.

[12] M. E. Davies and C. J. James, "Source separation using single channel ica," *Elsevier Signal Processing*, vol. 87, no. 8, pp. 1819–1832, 2007.

[13] N. Golyandina, V. Nekrutkin, and A. A. Zhigljavsky, *Analysis of time series structure: SSA and related techniques*. CRC press, 2001.

[14] A. Hyvärinen, J. Karhunen, and E. Oja, *Independent component analysis*. John Wiley & Sons, 2004, vol. 46.

[15] L. Kaufman and P. J. Rousseeuw, *Finding groups in data: an introduction to cluster analysis*. John Wiley & Sons, 2009, vol. 344.

[16] H. Ding, G. Trajcevski, P. Scheuermann, X. Wang, and E. Keogh, "Querying and mining of time series data: experimental comparison of representations and distance measures," *VLDB*, vol. 1, no. 2, pp. 1542–1552, 2008.

[17] Z. H. Hu, Y. I. Nechayev, P. S. Hall, C. C. Constantinou, and Y. Hao, "Measurements and statistical analysis of on-body channel fading at 2.45 ghz," *IEEE Antennas and Wireless Propagation Letters*, vol. 6, pp. 612–615, 2007.

[18] M. Kim and J.-I. Takada, "Statistical model for 4.5-ghz narrowband on-body propagation channel with specific actions," *IEEE Antennas and Wireless Propagation Letters*, vol. 8, pp. 1250–1254, 2009.

[19] Y. Xiong and F. Quek, "Hand motion gesture frequency properties and multimodal discourse analysis," *Springer International Journal of Computer Vision*, vol. 69, no. 3, pp. 353–371, 2006.

[20] P. Zhang, P. Hu, V. Pasikanti, and D. Ganesan, "Ekhonet: high speed ultra low-power backscatter for next generation sensors," in *Proc. ACM MobiCom*, 2014, pp. 557–568.

[21] Y. Wang, J. Yang, Y. Chen, H. Liu, M. Gruteser, and R. P. Martin, "Tracking human queues using single-point signal monitoring," in *Proc. ACM MobiSys*, 2014, pp. 42–54.

[22] T. Vu, A. Baid, S. Gao, M. Gruteser, R. Howard, J. Lindqvist, P. S-pasojevic, and J. Walling, "Distinguishing users with capacitive touch communication," in *Proc. ACM MobiCom*, 2012, pp. 197–208.

[23] C. Peng, G. Shen, Y. Zhang, and S. Lu, "Point&connect: intention-based device pairing for mobile phone users," in *Proc. ACM MobiSys*, 2009, pp. 137–150.

[24] Z. Sun, A. Purohit, R. Bose, and P. Zhang, "Spartacus: spatially-aware interaction for mobile devices through energy-efficient audio sensing," in *Proc. ACM MobiSys*, 2013, pp. 263–276.

[25] L. Zhang, X.-Y. Li, W. Huang, K. Liu, S. Zong, X. Jian, P. Feng, T. Jung, and Y. Liu, "It starts with igaze: Visual attention driven networking with smart glasses," in *Proc. ACM MobiCom*, 2014, pp. 91–102.

[26] M. Miettinen, N. Asokan, T. D. Nguyen, A.-R. Sadeghi, and M. Sobhani, "Context-based zero-interaction pairing and key evolution for advanced personal devices," in *Proc. ACM CCS*, 2014, pp. 880–891.

[27] L. Shi, M. Li, S. Yu, and J. Yuan, "Bana: body area network authentication exploiting channel characteristics," *IEEE Journal on Selected Areas in Communications*, vol. 31, no. 9, pp. 1803–1816, 2013.